Microstructure characterization of laser-deposited titanium carbide and zirconium-based titanium metal matrix composites

by O.F. Ochonogor*, C. Meacock†, S.L. Pityana*†, P.A.I. Popoola*, and J. Dutta Majumder‡

Synopsis

Laser metal deposition (LMD) is an additive manufacturing technique whereby a stream of metal powder is consolidated by a focused laser beam on the surface of a substrate or engineering component. The interaction zone between the laser beam and powder particles is scanned superficially, generating tracks of deposited material. The tracks are overlapped in a deposition strategy in accordance with slices of a CAD model. Successive layers of material are built up to fabricate a near net shape part. In this work, the technique is used to fabricate metal matrix composites (MMCs) by using an elementally blended feedstock combining metal and ceramic powders in the melt pool, which melt and solidify to create the required morphology. Ti6Al4V + TiC MMCs were produced with 10, 20, and 30 vol.% reinforcing ceramic, and Zr + TiC MMCs were fabricated with 10, 20, and 30 vol.% TiC. The deposited thin walls were analysed using optical microscopy, scanning electron microscopy (SEM) with energy dispersive spectroscopy (EDS), and indentation testing. In both systems, the analysis revealed the presence of partially melted TiC particles embedded in the metal matrix along with fine dendrites of re-solidified ceramic. The dendritic structures in the Ti-based composites were confirmed as TiC, whereas in the Zr-based composite the Zr metal reacts with the TiC to form ZrC, leaving Ti in solid solution. Both the MMCs show an increase in microhardness with increasing ceramic (carbide) content, reaching a peak $HV_{0.1}$ value of 500 in the Zr- based MMC and $HV_{0.1}$ of 550 in the Ti based MMC.

Keywords

laser metal deposition, metal matrix composites, Ti6Al4V, zirconium, titanium carbide, zirconium carbide.

Introduction

Throughout the history of manufacturing, the processes utilized can be designated as either formative, where a material is shaped into a required form, or subtractive, where a material is removed in order to realize the intended part. During the past thirty years, a third category of process has emerged whereby an object is produced by the controlled addition of material to form successive layers corresponding to the sections of the desired structure. Additive processes of this nature are classified by a wide range of generic names, depending on the application. Rapid-prototyping is generally used when describing a process that produces a part for shape visualization or shape evaluation. Rapid-manufacture/tooling is used in producing one-of-a-kind or a production small series of parts for functionality testing or commercial production. In this work, the broad term additive manufacture will be used.

Laser metal deposition (LMD) is a method of depositing solid materials whereby metallic or ceramic powder particles from a powder stream are blown into a pool of molten material generated on a substrate by an incident laser beam. The powder particles melt and diffuse within the molten material. The powder stream/laser beam focal point is scanned over the substrate surface leaving a track of deposited material as the molten material solidifies. By repeating the process and displacing the scanning path horizontally along the substrate surface, coatings with unique mechanical and corrosive properties can be formed/produced[1–3].

This process has been used as a method of laser freeform fabrication, creating three-dimensional objects by overlapping layers of deposited material[4–6]. To create a part by LMD, computer-aided design (CAD) renderings of the object are converted to standard tessellation language (STL) files and sliced into layers corresponding to the height of a track deposited by the LMD system. The system successively deposits material in accordance with each STL layer, building a fully dense part[7].

* Department of Chemical and Metallurgical Engineering, Tshwane University of Technology, Pretoria, South Africa.
† National Laser Centre, CSIR, Pretoria, South Africa.
‡ Department of Metallurgical and Materials Engineering, Indian Institute of Technology, West Bengal, India.

Microstructure characterization of laser-deposited titanium carbide

LMD has been used to fabricate components from titanium alloys in the USA since the mid-1990s. The technique has been used to manufacture components from Ti6Al4V for the aerospace industry and to produce functionally graded components of titanium with refractory materials[8,9]. Other areas where titanium alloys find application are the marine and chemical industries, as they offer important advantages such as high strength–to-weight ratio and excellent resistance to corrosion, oxidation, and high-temperature oxidation. Various studies have investigated the microstructure and phase compositions of laser-deposited Ti6Al4V, generally concurring that the bulk of deposited material presents an α/β /martensitic microstructure within columnar prior β grains, and that the higher the power density used during the process, the coarser the columnar prior beta grains[10–12].

Titanium alloys exhibit poor tribological properties due to a comparatively low surface hardness and high coefficient of friction[13]. Hence, in order to enhance the superficial properties, coatings of ceramic-reinforced titanium matrix composites produced by LMD have been researched[14–18]. In this preliminary work, metal matrix composites (MMCs) of Ti6Al4V reinforced with TiC and Zr were deposited and characterized. Zr was selected as a matrix due to its comparatively high corrosion resistance.

Experimental method

Laser metal deposition equipment

The LMD system at CSIR is comprised of several components as shown in Figure 1.

A RofinSinar® 4 kW Nd:YAG laser was used to generate a beam that is coupled by a fibre optic to a focusing lens. A dual-hopper plasma spray type powder feeder supplied powder particles. The volume flow rate depends on the rotational speed of the powder supply channels that feed powder particles from the hoppers into a stream of inert argon gas. Powder particles were fed into a continuous coaxial deposition nozzle (Figure 2) which was aligned concentric with the laser beam. The nozzle acts to create a powder particle stream that flows into the spot of the focused laser beam. The nozzle is equipped with an inert-gas shroud chamber which provides an atmosphere of argon gas in the deposition area, preventing significant reaction between the liquid deposition material and atmospheric contaminants such as O_2 or N_2. The deposition head/optical system assembly was scanned in three dimensions by a KUKA robotic arm positioning system.

The LMD system was used to deposit Ti6Al4V + TiC and Zr + TiC MMCs with different relative volume fractions of dispersoids. The compositions used were: Ti6Al4V + 10–30 vol.% TiC (at an interval of 10 vol.% TiC) and Zr + 10–30 vol% TiC (at an interval of 10 vol.% TiC). The process was facilitated by using flow from two powder feed hoppers, containing Ti6Al4V and TiC particles, and Zr, TiC particles respectively, which were combined to generate a powder stream with the required volume fractions. Spheroidal gas-atomized Ti6Al4V powder particles with a size distribution of 45–75 μm and milled TiC particles with a size distribution of 45–125 μm and an irregular morphology were used. Zirconium powder particles produced by milling to a size range of 32 μm to 125 μm were also used.

Depositions were conducted on 7 mm thick Ti6Al4V substrate prepared by sandblasting and subsequent cleaning with ethanol. The laser beam was focused to produce a beam spot of 1 mm diameter and a beam power of 750 W was used. The laser beam was scanned at a speed of 10 mm.s-1 over a length of 25 mm. Successive layers of material were deposited and after each pass the deposition head was offset by 0.4 mm normal to the substrate surface to maintain powder and beam focusing conditions.

Materials characterization

Metatallographic analyses were started by cutting, grinding, polishing, and etching the surfaces. The depositions were

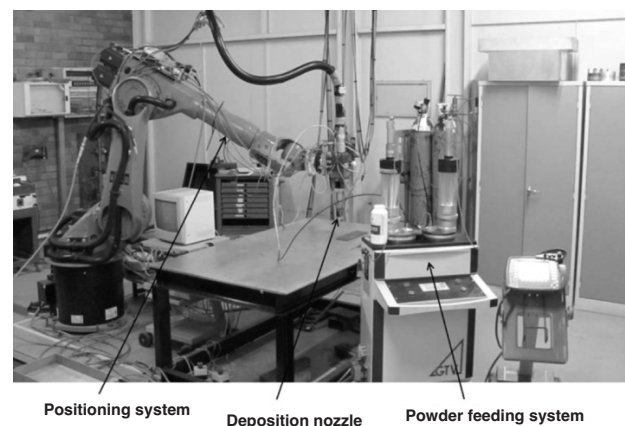**Positioning system**   **Deposition nozzle**   **Powder feeding system**

Figure 1—Photograph of the laser metal deposition facility
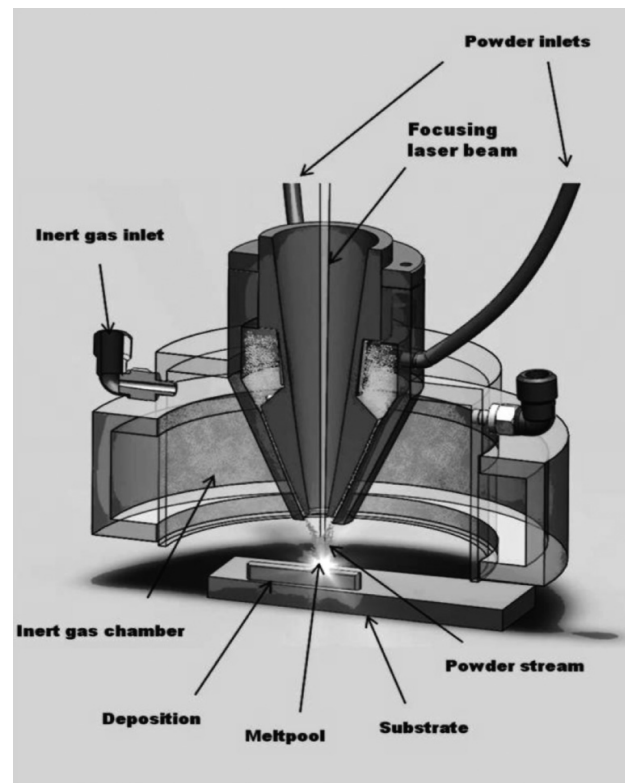

Figure 2—Schematic diagram of coaxial deposition nozzle (CSIR)

Microstructure characterization of laser-deposited titanium carbide

laterally sectioned, mounted, ground, and successively polished with finer SiC grit papers then finally polished using colloidal silica. The etchant used was Kroll's Reagent, which consists of distilled water (92 mℓ), HNO3 (6 mℓ), and HF (2 mℓ) for less than 15 seconds.

Optical and electron microscopy and EDS analysis were conducted on each sample. Microhardness measurements were conducted on each sample with a load of 100 g.

Results and discussion

Ti-MMCs

Figure 3a shows an optical macrograph of a section through a laser-deposited titanium-based thin-wall MMC. This sample shows an absence of porosity and low levels of variation in deposition geometry throughout the part. Figure 3b shows a photograph of the un-sectioned structure. There is a slight variation in the geometries of the deposited walls with respect to volume fraction of TiC. The build rate per layer is highest for 10 vol.% TiC at 0.4 mm, but decreasing linearly with composition to 0.32 mm at 50 vol.% TiC. The width of the deposition remains fairly uniform at approximately 2 mm.

Figure 4 shows the presence of a morphological gradient between the lower layers of the wall and upper layers of the deposited titanium parts. At approximately 60–75 per cent of the build height there is a transition from the lower region, where partially melted TiC particles are well dispersed throughout the Ti metal matrix, to the lower region, where TiC particles appear to have been entirely melted. Figures 5 and 6 show optical micrographs at higher magnifications taken in the lower and upper regions of the deposits respectively. In all deposits, the metal matrix is comprised of columnar prior beta grains, which are remnants of the high-temperature beta phase that would form on initial solidification from the melt. Within these morphological features, the presence of alpha martensite needles is visible. In the lower regions of the walls, the metal matrix contains two types of reinforcing ceramics: partially melted TiC particles and dendritic TiC that has re-solidified from the meltpool on solidification. In the upper regions of the walls, only dendritic TiC is observed. With increasing TiC content, the dendritic TiC becomes more prevalent. In the samples with lower TiC content, the dendrites are comparatively thin, less than 2 μm, with little formation of secondary dendrite arms. With increasing TiC content the dendrites become coarser, forming secondary and ternary dentrite arms. Figure 7 shows an EDS
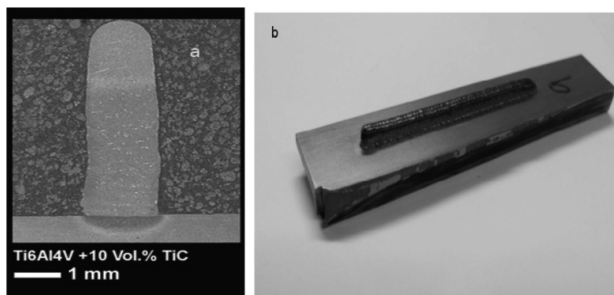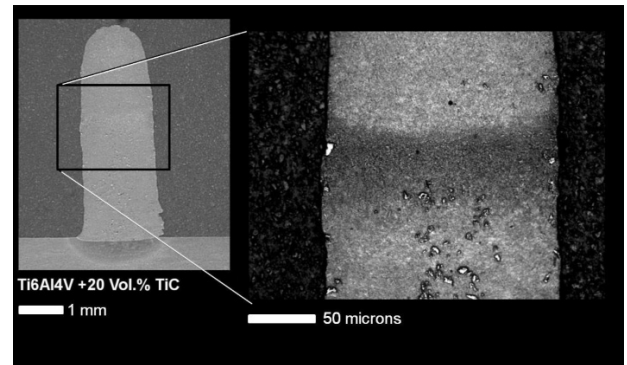

Figure 4—Optical macro- and micrographs showing microstructure transition occurring in laser-deposited MMCs
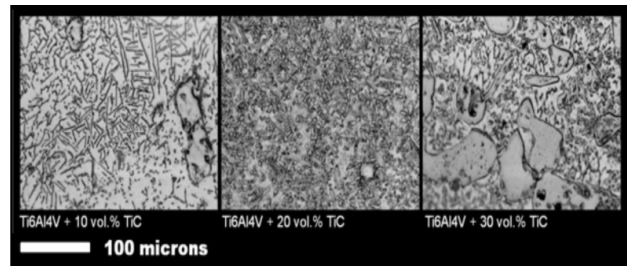

Figure 5–Optical micrographs showing microstructure morphology close to the substrate in laser deposited MMCs
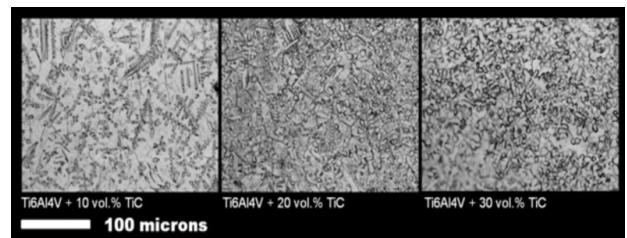

Figure 6–Optical micrographs showing microstructure morphology close to the wall apex in laser-deposited MMCs
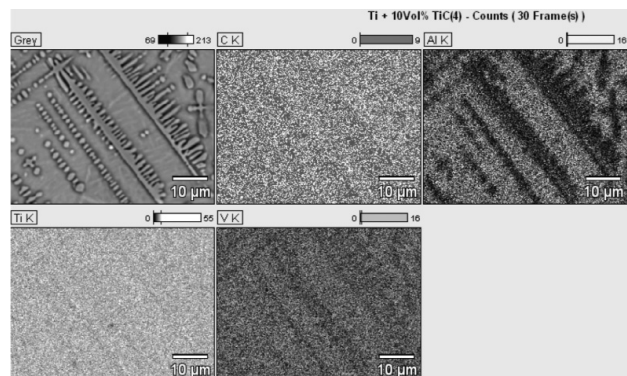

Figure 3—(a) Optical macrograph of a cross-section of laser-deposited MMC on Ti6Al4V substrate (b) photograph of Ti6Al4V MMC

Figure 7–EDS element map of dendritic TiC and martensitic Ti6Al4V matrix

element map of TiC dendrites within a martensitic matrix, where the dendrites are seen to be rich in carbon and the matrix rich in vanadium and aluminium, which are evenly dispersed in solid solution within the martensite matrix.

The morphological variation between the differing regions of the deposited walls can be attributed to the varying heat flux conditions occurring during the deposition of a thin wall by LMD. At the onset, deposition occurs on a substrate at ambient temperature where heat is easily conducted to the bulk of the substrate. As the process continues, each successive layer is deposited onto previously deposited and progressively hotter material. The increased temperatures mean less beam energy is required to melt the metal matrix and more is available to melt the ceramic TiC particle hence with increasing layers the probability of retaining partially melted TiC particles diminishes. It is preferable to have a homogenous deposition microstructure, and hence further work will be conducted to examine the effect of ceramic particle size on deposition morphology. For structural applications, finer reinforcing particles typified by the dendrite structures displayed in this work are preferable, and thus it would be necessary to use TiC with a narrower particle size distribution. Conversely for applications where wear resistance is a priority, larger reinforcements such as the partially or un-melted particles are preferable. These morphologies would be achieved by utilizing ceramic particles with wider particle size distributions.

Zr-MMCs

Figure 8 shows an optical macrograph of a laser-deposited zirconium MMC. There is porosity present, but a slightly increased surface roughness arising from the irregular shape of the milled Zr powder particles is observed. The build rate was approximately 0.3 mm for each of the ten deposited layers, and the width was approximately 2 mm.
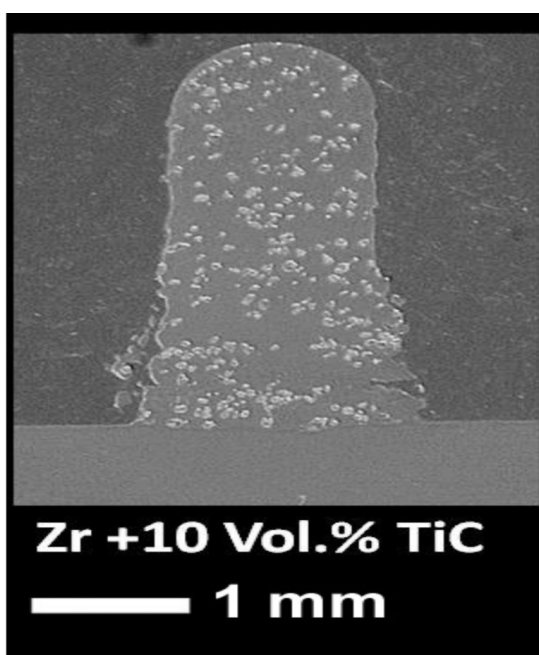
Figure 9 shows optical micrographs of Zr MMCs with 10, 20, and 30 vol.% TiC additions. The microstructures show a matrix of zirconium, which has formed a cellular structure on solidification. Embedded within the matrix are un-melted TiC particles and ceramic which has resolidified in dendritic form. Unlike the Ti-based deposits, the microstructure morphology remains fairly consistent throughout with un-melted particles. As seen in Figures 10(b) and 10(a), which show a backscattered electron image of the deposited Zr + 30 vol.% MMC, the titanium has decomposed into a secondary heavier phase which formed dendrites. When analysed using EDS spectroscopy, as shown in Figures 11 and 12, the resolidified material was identified as ZrC, which would have formed due to the reaction $TiC + Zr \rightarrow ZrC + Ti$. The titanium is seen to diffuse into the zirconium matrix and is concentrated at the interface between the ceramic and metal.

Hardness values for the two sets of samples (Figure 13 and 14) show an increase in hardness with increasing TiC content, with the highest value of 550 $HV_{0.1}$ for the Ti6Al4V and 500 $HV_{0.1}$ for the Zr MMC. The hardness should correlate with an increase in wear resistance and a decrease in ductility.
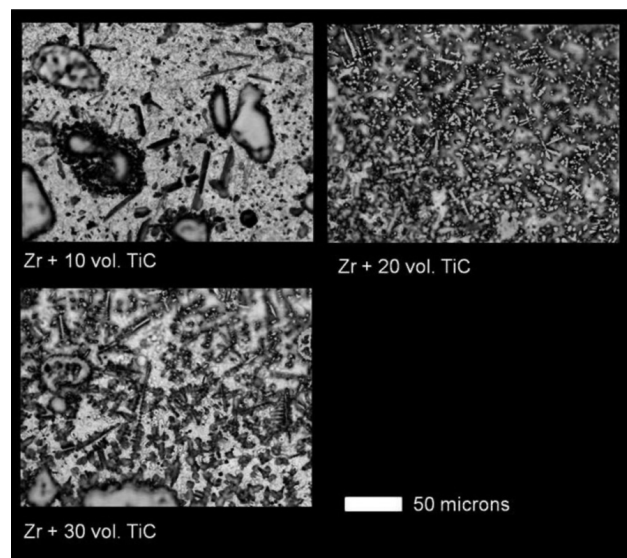

Figure 9–Optical micrographs showing Zr / TiC microstructure morphology in laser-deposited MMCs
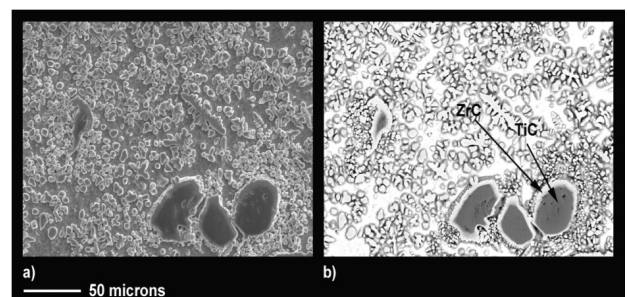

Figure 8–Optical macrograph of laser-deposited metal matrix composite on Ti6Al4V substrate

Figure 10–SEM Micrograph showing the decomposition of TiC particles a) Secondary electron imaging, b) Backscattered electron imaging
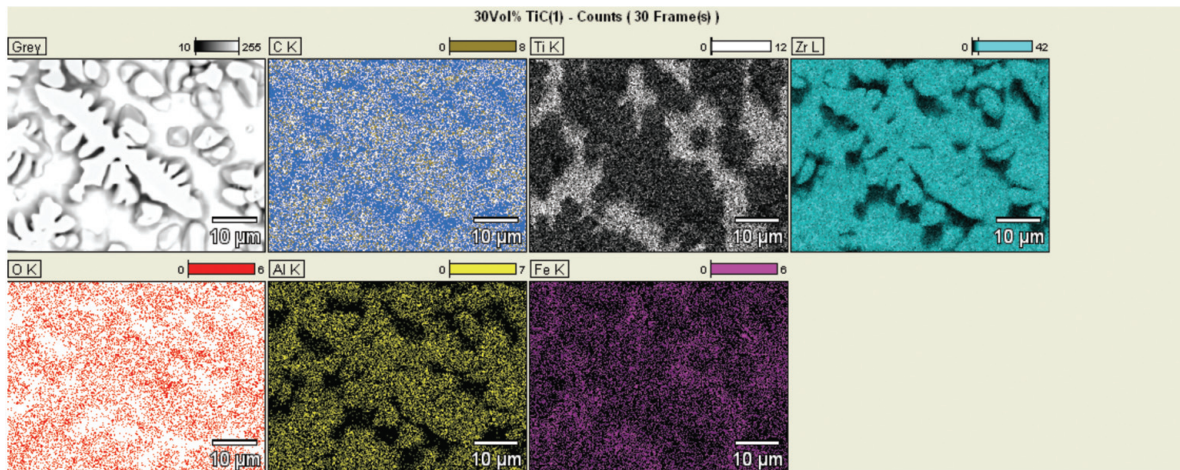
Figure 11—EDS element map of dendritic ZrC and dentritic TiC matrix

Figure 12—Backscattered SEM micrograph showing decomposition of TiC
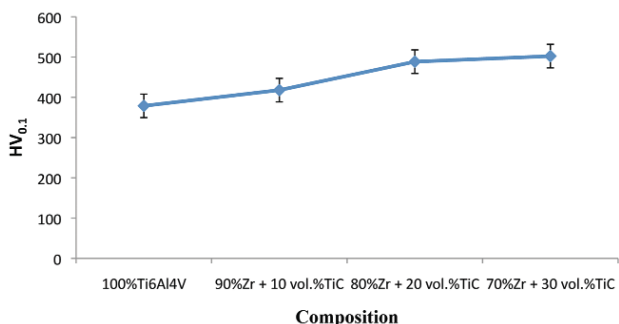

Figure 13–Average hardness measurements of laser-deposited Ti-TiC MMCs with respect to increasing TiC composition

Figure 14—Average hardness measurements of laser-deposited Zr-TiC MMCs with respect to increasing TiC composition

➤ Optical macrographs of the deposits showed no evidence of porosity and low levels of variation in the deposition geometry were seen
➤ In Ti-based MMCs, fine TiC dendrites were formed in certain regions of the deposits due to melting and re-solidification of TiC particles
➤ In Zr-based MMCs, TiC particles decomposed to form ZrC particles
➤ The hardness of the deposits increased with increase in ceramic content of the mixture, which could relate to an increase in wear resistance
➤ The hardness increased to approximately 500 HV0.1 for Zr MMC, and 550 HV0.1, for Ti MMC reinforced with 30 vol.% ceramic.

Further work will be done to investigate the wear and electrochemical mechanism of these systems. However, it is advisable to examine the wear using a larger coated surface, which is the intention of further investigation

Conclusions

The following conclusions can be drawn from the results of this study.
➤ The laser metal deposition technique was successfully used to manufacture Ti/TiC and Zr/TiC/ZrC metal matrix composite thin walls
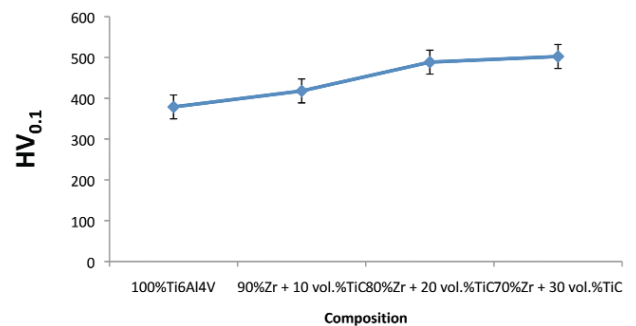
Acknowledgements

Microstructure characterization of laser-deposited titanium carbide

References

1. VREELING, J.A., OCELIK, V., HAMSTRA, G.A., PEI, Y.T., and DE HOSSON, J.M. Insitu microscopy investigation of failure mechanisms in Al/SiC metal matrix composite produced by laser embedding. *Scripta Materialia*, vol. 42, 2000, pp. 589–95.

2. VILAR, R. Laser cladding. *Journal of Laser Applications*, vol. 11, no. 2, 1999. pp. 64–79.

3. LIN, W.C. and CHEN, C. Characteristics of thin surface layers of cobalt based alloys deposited by laser cladding. *Surface and Coatings Technology*, vol. 200, 2005. pp. 4557–4563.

4. DUTTA MAJUMDAR, J. and MANNA, I. Laser materials processing. *International Materials Reviews*, vol. 56, 2011, pp. 341–387.

5. DUTTA MAJUMDAR, J. and LI, L. Development of titanium boride (TiB) dispersed titanium (Ti) matrix composite by direct laser cladding. *Materials Letters*, vol. 64, 2010, pp. 1010–1012.

6. WU, X. and MEI, J. Near net shape manufacturing of components using direct laser fabrication technology. *Journal of Materials Processing Technology*, vol. 135, 2003. pp. 266–270.

7. KULKARNI, P., MARSAN, A., and DUTTA, D. A review of process planning techniques in layered manufacturing. *Journal of Rapid Prototyping*, vol. 6, no. 1, 2000. pp. 18–35.

8. ARCELLA, F.G. and FROES, F.H. Producing titanium aerospace components from powder using laser forming. *Journal of Metals*, vol. 52, no. 5, 2000. pp. 28–30.

9. COLLINS, P. C., BANERJEE, R., BANERJEE, S., and FRASER, H.L. Laser deposition of compositionally graded titanium vanadium and titanium-molybdenum alloys. *Materials Science and Engineering*, vol. 352, 2001. pp. 118–28.

10. KOBRYN, P.A., MOORE, E.H., and SEMIATIN, S.L. The effect of laser power and traverse speed on microstructure, porosity and build height in laser deposited. Ti–6Al–4V. *Scripta Materialia*, vol. 43, 2000. pp. 299–305.

11. KLINGBEIL, N.W., KOBRYN, P.A., FRASER, H.L., and SEARS, J.W. Effects of process variables and size scale on solidification microstructure in laser-based solid freeform fabrication of Ti–6Al–4V. *Solid Freeform Fabrication Symposium*, 2004. http://www.dtic.mil/cgi-bin/GetTRDoc?AD=ADP020465.

12. ERHARD, B. and DANIEL, G. Microstructure of additive layer manufactured Ti–6Al–4V after exceptional post heat treatments. *Materials Letters*, vol. 81, 2012. pp. 84–87.

13. LAN, Y.Q., GUANG, Y., WEI, W., MING, T., and XING, L.W. Application of laser metal deposition for fabrication of titanium matrix wear-resistant coating and its wearing performance. *Applied Mechanics and Materials*, vol. 44–47, 2010. pp. 316-320.

14. WATKINS, K.G. Achieving the potential of direct fabrication with lasers. Proceedings of the 3rd International Conference on Laser Asssisted Net Shaping (LANE 2001) Erlangen, August 2001. Meisenbach-Verlag Bamberg. pp. 25–38.

15. LIU, W. and DUPONT, J.N. Fabrication of functionally graded TiC/Ti composites by laser engineered net shaping. *Scripta Materialia*, vol. 48, 2003. pp. 1337–1342.

16. DINDA, G.P., SONG, L., and MAZUMDER, J. Fabrication of Ti-6Al-4V scaffolds by direct metal deposition. *Metallurgical and Materials Transactions*, vol 39A, 2008. pp. 2914–2922.

17. JUN, L., ZHISSHUI, Y.U., HUIPING, W., and MANPING, L. Microstructural characterisation of titanium matrix composite coatings reinforced by in situ synthesized TiB+TiC fabricated on Ti6Al4V by laser cladding. *Rare Metals*, vol. 29, 2010. pp. 465–472.

18. ZHENG, B., SMUGERESKY, J.E., ZHOU, Y., BAKER, D., and LAVERNIA, E.J. Microstructure and properties of laser deposited Ti6Al4V metal matrix composites using Ni coated powder. *Metallurgical and Materials Transactions*, vol. 39A, 2008. pp. 1196–1205. ◆